

Article

Scattering of Ultrashort X-ray Pulses from Oriented NV Centers in the Diamond Structure

Dmitry Makarov ^{*}, Marat Eseev , Eugeny Gusarevich, Viktor Matveev, Ksenia Makarova and Mark Borisov

Higher School of Natural Sciences and Technologies, Northern (Arctic) Federal University, Nab. Severnoi Dviny 17, 163002 Arkhangelsk, Russia; m.eseev@narfu.ru (M.E.); e.gusarevich@narfu.ru (E.G.); mezon98@mail.ru (V.M.); k.makarova@narfu.ru (K.M.); borisov.m@edu.narfu.ru (M.B.)

* Correspondence: makarovd0608@yandex.ru

Abstract: It is well known that the basis of diffraction analysis of matter is scattering, including the scattering of ultrashort laser pulses. In the theory of scattering of ultrashort pulses, the pulse duration parameter is usually not taken into account, which leads to some error. This error may be more significant than the considered effects in the scattering of the pulse on the studied structure. In this paper, it is shown that the pulse duration parameter should be taken into account when scattering X-ray pulses on oriented diamonds with NV centers. It is shown that the scattering spectra can be used to judge the orientation of NV centers in the diamond structure. The obtained results may be very different from the widely used theory of diffraction analysis, which confirms the necessity of taking into account the pulse duration parameter in the diagnosis of complex structures.

Keywords: diamond; NV centers; orientation of NV centers; ultrashort pulse; scattering; X-ray diffraction analysis.



Citation: Makarov, D.; Eseev, M.; Gusarevich, E.; Matveev, V.; Makarova, K.; Borisov, M. Scattering of Ultrashort X-ray Pulses from Oriented NV Centers in the Diamond Structure. *Crystals* **2024**, *14*, 193. <https://doi.org/10.3390/cryst14020193>

Academic Editors: Alessandra Toncelli, Felix Chukhovskii, Konarev V. Petr and Vladimir Vladimirovich Volkov

Received: 23 November 2023

Revised: 16 January 2024

Accepted: 13 February 2024

Published: 14 February 2024



Copyright: © 2024 by the authors. Licensee MDPI, Basel, Switzerland. This article is an open access article distributed under the terms and conditions of the Creative Commons Attribution (CC BY) license (<https://creativecommons.org/licenses/by/4.0/>).

1. Introduction

X-ray diffraction analysis of matter (XRD) using ultrashort laser pulses (USPs) is currently gaining great relevance [1–3]. First of all, this development of the physics of ultrashort pulses was facilitated by the emergence of new installations generating such pulses [4–8]. Such sources primarily include free electron lasers (XFELs) [9], which can generate very high peak and average powers of laser radiation in the X-ray frequency range. The generation of attosecond X-ray pulses by XFELs is currently being reported [10,11]. The possibility of creating zeptosecond pulses is reported [12]. Achieving a subfemtosecond barrier with high peak power makes it possible to study excitation in a molecular system: the movement of valence electrons with high temporal and spatial resolution, for example, [13]. Indeed, with the help of such USPs, it is possible to study the structure of a substance with high temporal and spatial resolution, since it is technically possible to carry out such studies. Despite this, there is a need for new theoretical approaches that take into account the specific interaction of such USPs with complex structures, including promising materials that can be used in quantum technologies.

One of the most interesting materials in quantum technologies is diamonds with NV centers. An NV center (nitrogen vacancy center) in diamonds is one of many point defects in diamonds that appear when a carbon atom is removed from a lattice site and the resulting vacancy binds to a nitrogen atom. The uniqueness of the NV defect is due to the fact that the spins of individual central electrons can be easily manipulated by magnetic, light, electric and microwave fields, which makes it possible to write quantum information (qubits) onto the spin of the central nucleus. What is especially important is that such manipulations are possible even at room temperature [14,15]. Of particular importance for quantum technologies are the so-called NV⁻ centers (usually denoted as NV), which have an additional electron located at the vacancy site and form a spin $S = 1$ pair with one of the vacancy electrons. This leads to improvements in technologies for creating and

diagnosing materials based on synthetic diamond plates with NV centers (color centers). Of great interest are defects in diamonds created from layers of NV centers. This is due to the fact that layers localized in a crystal make it possible to produce a quantum sensor for the magnetometry of objects with high spatial resolution. The layers can also be used in diamond quantum electronics elements [16]. These layers can be created in several ways. First, nitrogen is implanted into a crystal grown by the high-pressure–high-temperature method (HPHT) during growth; then, the crystal is irradiated with heavily charged particles (for example, protons) at a certain energy. Due to the crystalline lattice and subsequent annealing, a thin layer of NV centers is formed [17]. Secondly, they use the chemical vapor deposition method (CVD) technology [18]. In this case, layers of nitrogen are formed during the growth of the wafer, and then the wafer is irradiated with electrons and annealed to create vacancies. To use such NV centers in quantum technologies, it is necessary to be able to determine not only their presence and quantity in the crystal structure but also the orientation of these centers. Determining their orientation is quite difficult, although it is possible using the optically detected magnetic resonance (ODMR) method, since the NV center is sensitive to the external magnetic field [19]. Due to the symmetry of the crystal, there are four possible orientations of the NV axis in the diamond lattice: $111, \bar{1}\bar{1}\bar{1}, \bar{1}\bar{1}1, 1\bar{1}\bar{1}$. Determining these directions is a non-trivial and quite complex task.

Currently, ultrashort laser pulses are increasingly being used in the diffraction analysis of matter. Such ultrashort pulses make it possible not only to determine the structure of matter but also the dynamic processes that occur in them. The diffraction analysis of such structures with ultra-high spatial and temporal resolution is a promising direction in modern physics. Femto- and especially attosecond scattering processes on such structures with time resolution have been little studied and are currently being actively developed [5,7,8,20–28]. Typically, the scattering of X-rays by various periodic and complex structures is described as the scattering of plane monochromatic waves of infinite duration in time [3,29]. This means that the duration of such USPs when scattering on such structures is not taken into account, which leads to an inaccurate use of known approaches in XRD [3,5]. Such inaccuracies can have a large error, which will lead to incorrect “decoding” of the structure under study. Indeed, it was recently modeled that the scattering of attosecond USPs on DNA structures can differ significantly from the previously known XRD theory [30]. Also, if you do not take into account the duration of the USP, then you can incorrectly determine various mutations and defects in DNA [31]. Thus, the study of USP scattering on a diamond with a given orientation of NV centers, taking into account the USP duration, is an urgent task. Indeed, the elemental composition of a diamond crystal with different orientations of NV centers is the same, which means that the scattering spectra from such NV centers differ by a small amount, and if the error of the calculation method is quite large, then the effect from the orientation of NV centers will not be noticeable. Thus, theory and calculations are needed, where the pulse duration will be an important parameter of the theory under consideration.

In this work, the scattering of USPs on diamonds with different orientations of NV centers is studied. It is shown that using USP, it is possible to determine the orientation of NV centers in the crystal structure. It is also shown that pulse duration is an important parameter, especially when using attosecond pulses, and the use of previously known XRD theory can lead to large errors that are more significant than the differences in the scattering spectra of USPs at different orientations of NV centers.

Furthermore, we will use the atomic system of units: $\hbar = 1$; $|e| = 1$; $m_e = 1$, where \hbar is the Dirac constant, e is the electron charge, and m_e is the electron mass.

2. USP Scattering on Oriented NV Centers

Let us consider the scattering of USPs incident in the direction \mathbf{n}_0 onto oriented NV centers in the diamond structure. As an example, let us consider scattering on NV centers located in a plane for all four directions of their orientation. Let us define orientation 1,

presented in Figure 1; orientation 2 shown in Figure 2; orientation 3 presented in Figure 3; and orientation 4 presented in Figure 4.

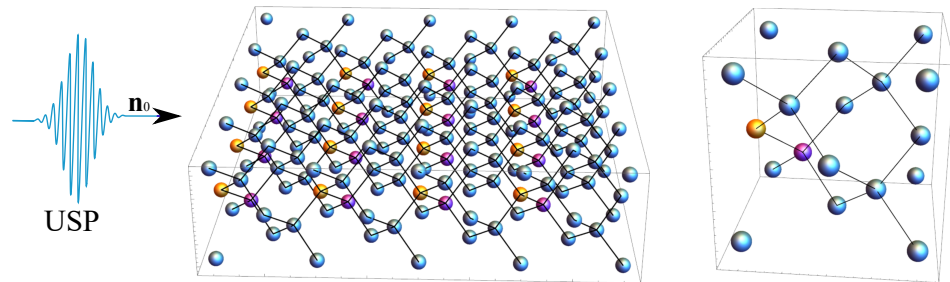


Figure 1. USP incident on a diamond structure with oriented NV centers (orientation 1) is presented. The diamond structure is defined by 16 unit cells of diamonds (4×4). Blue circles are carbon atoms, purple circles are nitrogen atoms, and yellow circles are vacancies. On the right is a unit cell with an NV center with orientation 1.

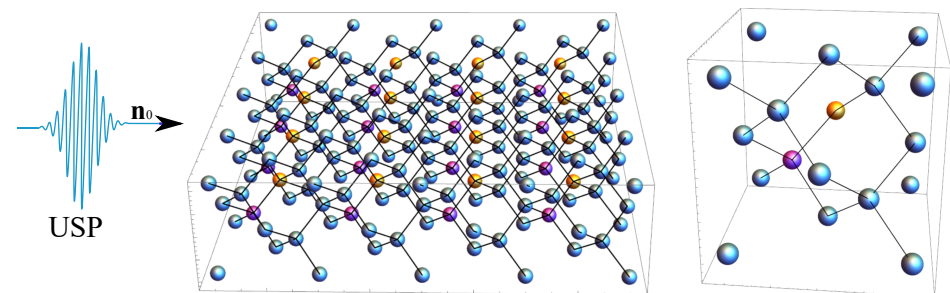


Figure 2. The same as in Figure 1 but with orientation 2.

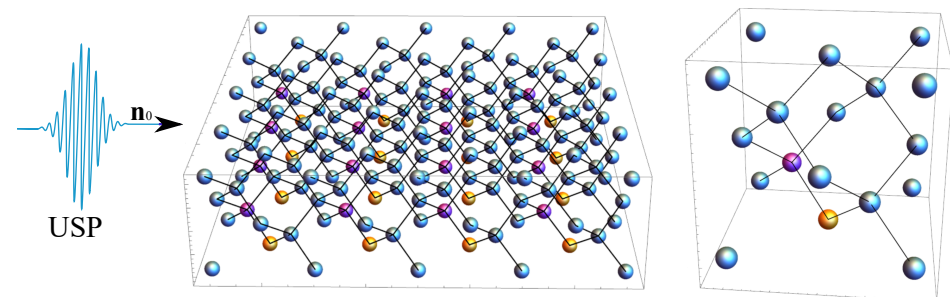


Figure 3. The same as in Figure 1 but with orientation 3.

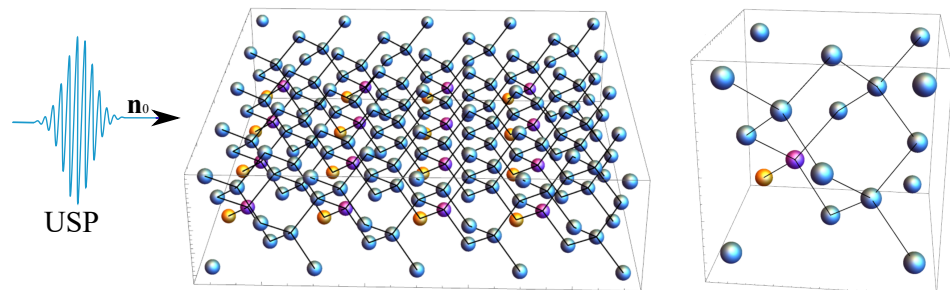


Figure 4. The same as in Figure 1 but with orientation 4.

In the works [24,25,30–32], it was shown that when using the sudden disturbance approximation, it is possible to obtain expressions for calculating scattering spectra taking into account the duration of the incident USP. The special role of the pulse duration during its scattering is determined by attosecond pulses; i.e., such pulses can give a large difference in the scattering spectra when using the previously known theory and the theory

developed in these works. These are the pulses that will be used in this work. Let us add that the sudden perturbation approximation works well for pulse durations $\tau \ll \tau_a$ ($\tau_a \sim 1$ is atomic time). Also, when using the sudden disturbance approximation, the theory coincides with the previously known scattering theory in the case of a long pulse (τ these are femtosecond pulses and even longer) [24,32]. This coincidence is easily explained due to the fact that the previous scattering theory is based on the fact that an electron in the field of X-ray radiation can be considered free even if it is located in an atom. The sudden perturbation approximation is a more general approximation than the free electron approximation [32], but in the non-relativistic case, it is close to it. However, even with femtosecond pulses, a difference between the previously known scattering theory and experiment can be observed at very strong ultrashort pulse intensities. For example, in the work [33], they used a pulse of tens of femtoseconds and an intensity close to 10^{20} W/cm², where such differences were shown. In the field of such an intense pulse, the electrons in an atom do not simply oscillate in the USP field, but the electron density of the atoms changes during the action of the pulse and it shifts by a certain amount. The shift in such electron density contributes to the scattering spectra. The theory we will use here does not take into account such displacements, which can be estimated as $\delta r \sim \frac{eE_0}{m} \tau^2$ (displacement in a strong field). If this displacement is many times smaller than the Bohr radius a ($\delta r/a \ll 1$), then it can be ignored. It can be seen that for femtosecond pulses, the bias begins to play a role at approximately $\sim 10^{20}$ W/cm² intensities. With attosecond pulses, even with more intense pulses, the displacement can be neglected.

Furthermore, we will consider the pulse to be spatially inhomogeneous, i.e., let us choose the electromagnetic field strength USP in the general form $\mathbf{E}(\mathbf{r}, t) = \mathbf{E}_0 h(t - \mathbf{n}_0 \mathbf{r}/c)$, where \mathbf{E}_0 is the field amplitude, $h(t - \mathbf{n}_0 \mathbf{r}/c)$ is an arbitrary function that determines the shape of the USP, and c is the speed of light (in a.e. $c \sim 137$). We will not consider USP fields to be so strong that nonlinear effects appear. These effects begin to appear when the USP magnetic field also needs to be taken into account. As was shown in the works [24,32], the USP magnetic field can be ignored at intensities $I \ll 10^{25}$ W/cm². In this case, as was shown in [30,31], scattering spectra (scattered USP energy per unit solid angle) can be represented as

$$\frac{d\varepsilon}{d\Omega_{\mathbf{k}}} = \frac{[\mathbf{E}_0 \mathbf{n}]^2}{(2\pi)^2 c^3} \tau \int_{-\infty}^{\infty} |\tilde{f}(x)|^2 dx \left[\sum_{i=1}^s N_{e,i} N_{A,i} (1 - |F_i(\mathbf{p}_0)|^2) + \sum_{i,j=1}^s \gamma_{i,j}(\mathbf{p}_0, \mathbf{p}_\tau) N_{e,i} N_{e,j} F_i(\mathbf{p}_0) F_j^*(\mathbf{p}_0) \right],$$

$$\gamma_{i,j}(\mathbf{p}_0, \mathbf{p}_\tau) = \sum_{A_i, A'_j} e^{-i\mathbf{p}_0(\mathbf{R}_{A_i} - \mathbf{R}_{A'_j})} \frac{\int_{-\infty}^{\infty} |\tilde{f}(x)|^2 e^{-ix\mathbf{p}_\tau(\mathbf{R}_{A_i} - \mathbf{R}_{A'_j})} dx}{\int_{-\infty}^{\infty} |\tilde{f}(x)|^2 dx}. \quad (1)$$

where $\mathbf{p}_0 = \frac{\omega_0}{c}(\mathbf{n} - \mathbf{n}_0)$ has the meaning of a recoil impulse at the carrier frequency ω_0 during USP scattering, and $\mathbf{p}_\tau = \frac{1}{c\tau}(\mathbf{n} - \mathbf{n}_0)$; $h = e^{-i(\omega_0 t - \mathbf{k}_0 \mathbf{r})} f((t - \mathbf{n}_0 \mathbf{r}/c)/\tau)$, where the f function defines the USP profile. Then, we obtain $\tilde{f}((\omega - \omega_0)\tau) = \int_{-\infty}^{\infty} e^{-i(\omega - \omega_0)\tau\eta} f(\eta) d\eta$ as the Fourier transform of the function $f(\eta)$; $N_{e,i}$ is the number of electrons in the atom i variety; $N_{A,i}$ is the number of atoms i variety; and $F_i(\mathbf{p}_0) = \frac{1}{N_{e,i}} \int \rho_{e,i}(\mathbf{r}) e^{-i\mathbf{p}_0 \mathbf{r}} d^3\mathbf{r}$ is the form factor of the i atom of the variety with electron density $\rho_{e,i}(\mathbf{r})$. The parameter s is the number of different kinds of atoms in the system. In our case, s can be considered equal to 2, since we are considering two independent atoms: carbon (C) and nitrogen (N). It should be taken into account that the place where there is a vacancy is empty, i.e., there are no atoms there.

Next, we will use the model of independent atoms. In this model, the entire crystal or molecule consists of individual neutral, non-interacting atoms. Indeed, such a model can be applied due to the fact that the bulk of the electrons on which the USP is scattered are not valence electrons, and there are significantly more of them than electrons involved in

interatomic bonds. Thus, we will further use the well-known model of electron density distribution in atoms [34]. The electron density of such atoms $\rho_{e,i}(\mathbf{r}) = \frac{N_{e,i}}{4\pi r} \sum_{k=1}^3 A_{k,i} \alpha_{k,i}^2 e^{-\alpha_{k,i} r}$, where $A_{k,i}, \alpha_{k,i}$ are constant coefficients (for all varieties of atoms with number i) defined in [34]. The result is a simple expression for $F_i(\mathbf{p}_0) = \sum_{k=1}^3 \frac{A_{k,i} \alpha_{k,i}^2}{p_0^2 + \alpha_{k,i}^2}$.

Let us choose the form of the falling USP in the form of a Gaussian form $h(t) = e^{-i(\omega_0 t - \mathbf{k}_0 \mathbf{r})} e^{-\alpha^2 (t - \mathbf{n}_0 \mathbf{r}/c)^2}$, where $\alpha = 1/\tau$ (τ is the pulse duration), $\mathbf{k}_0 = \mathbf{n}_0 \omega_0/c$. Let us add that the shape of the pulse can be chosen arbitrarily depending on the task at hand. In the case of X-ray pulses, multi-cycle pulses are usually used, i.e., where the number of fluctuations included in the USP is large. Mathematically, the multi-cycle pulse condition can be represented as $\omega_0 \tau \gg 1$. We choose a Gaussian pulse, since this type of pulse is the most common. For example, in [35], an exact description of the subcyclic pulse beam (SCPB) was found, where in the case considered in this article ($\omega_0 \tau \gg 1$), the solution has the form of a Gaussian pulse. In the multi-cycle pulse case, we obtain $\tilde{f}((\omega - \omega_0)\tau) = \sqrt{\pi} e^{-(\omega - \omega_0)^2/4\alpha^2}$; then, using Equation (1), it will turn out

$$\frac{d\varepsilon}{d\Omega_{\mathbf{k}}} = \frac{[\mathbf{E}_0 \mathbf{n}]^2}{2c^3 \alpha \sqrt{2\pi}} \left[\sum_{i=1}^s N_{e,i} N_{A,i} (1 - |F_i(\mathbf{p}_0)|^2) + \sum_{i,j=1}^s \gamma_{i,j}(\mathbf{p}_0, \mathbf{p}_\tau) N_{e,i} N_{e,j} F_i(\mathbf{p}_0) F_j^*(\mathbf{p}_0) \right],$$

$$\gamma_{i,j}(\mathbf{p}_0, \mathbf{p}_\tau) = \sum_{A_i, A'_j} e^{-i\mathbf{p}_0(\mathbf{R}_{A_i} - \mathbf{R}_{A'_j})} e^{-\frac{1}{2}(\mathbf{p}_\tau(\mathbf{R}_{A_i} - \mathbf{R}_{A'_j}))^2}. \quad (2)$$

In order to obtain the basic calculated Equation (1), the theory [24] was used, where an expression in general form was obtained for calculating the scattered energy per unit solid angle in a unit frequency interval regardless of the number of scattered centers and the intensity of incident radiation. To calculate this expression, we need the electron wave function in the USPs field, which was found in the work [32]. In the work [30], Equation (1) was obtained using [24,32] taking into account polyatomic structures and various atoms in these structures. When using Gaussian multi-cycle USPs, Equation (2) was obtained. Thus, details of the derivations and calculations of Equation (2) can be found in these works.

This expression contains characteristics responsible for the duration of the ultrashort pulse τ , which means that Equation (2) is more general in the theory of X-ray scattering than the well-known and widely used expression in scattering theory. If this duration parameter is made large, i.e., $\tau \rightarrow \infty$, and we take into account only the coherent term in scattering, then we obtain from Equation (2) the well-known expression for the scattering of long (monochromatic) X-rays [30]. The main difference between Equation (2) and the previously known theory is determined by the factor $\gamma_{i,j}(\mathbf{p}_0, \mathbf{p}_\tau)$, the analysis of which determines the difference between our theory and the previously famous one. As was shown in early works [25,30,31], the difference between the theory presented here and the previously known one is mainly observed when using attosecond and shorter pulses on certain types of structures. Analysis of the parameter $\gamma_{i,j}(\mathbf{p}_0, \mathbf{p}_\tau)$ provides a qualitative explanation of the influence of the pulse duration on the scattering spectra. If the spatial dimensions of the pulse $\sim c\tau$ are such that only part of the NV centers will fall into this size, then from this region of space, there can be scattering by this group of NV centers. All carbon atoms and NV centers that do not fall into the region of $\sim c\tau$ space are scattered independently of each other without diffraction. In the case of long-duration pulses, the space region is $c\tau \rightarrow \infty$, which means diffraction will be from all atoms and NV centers, i.e., from a very large area of space.

Next, we present calculations of USP scattering on the systems presented in Figures 1–4. The calculation of scattering spectra using the Formula (2) is shown in Figures 5–8. The pulse falls as shown in Figures 1–4 with photon energy $\hbar\omega_0 = 7.46$ keV, pulse duration $\tau = 10$ as. It should be added that the calculation is carried out numerically using the Wolfram Mathematica 12 program. For this, a code was written that calculated the scattering spectra using Equation (2). This code takes into account the spatial arrangement of carbon atoms and NV centers presented in Figures 1–4. A special feature of this code

is the optimization of the calculation time due to the parallel calculation of the data array. The time for calculating scattering spectra for each orientation did not exceed 20 s.

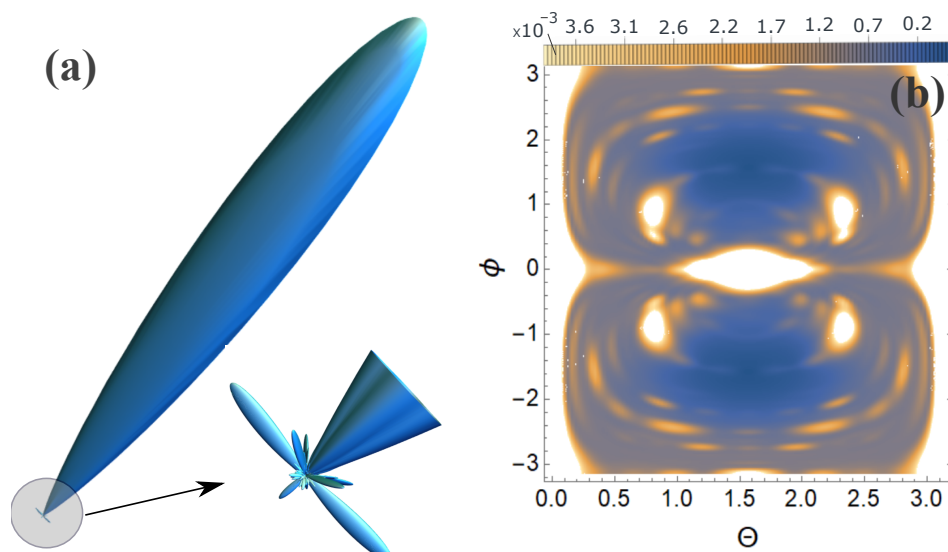


Figure 5. Scattering spectra are presented for orientation 1; see Figure 1: (a) 3D scattering spectra, where the main peak is directed in the direction of the incident pulse; (b) contour plot in a spherical coordinate system, where θ and ϕ are spherical angles, where ϕ is the azimuthal angle, and the z-axis is directed perpendicularly upward to the lattice plane Figure 1.

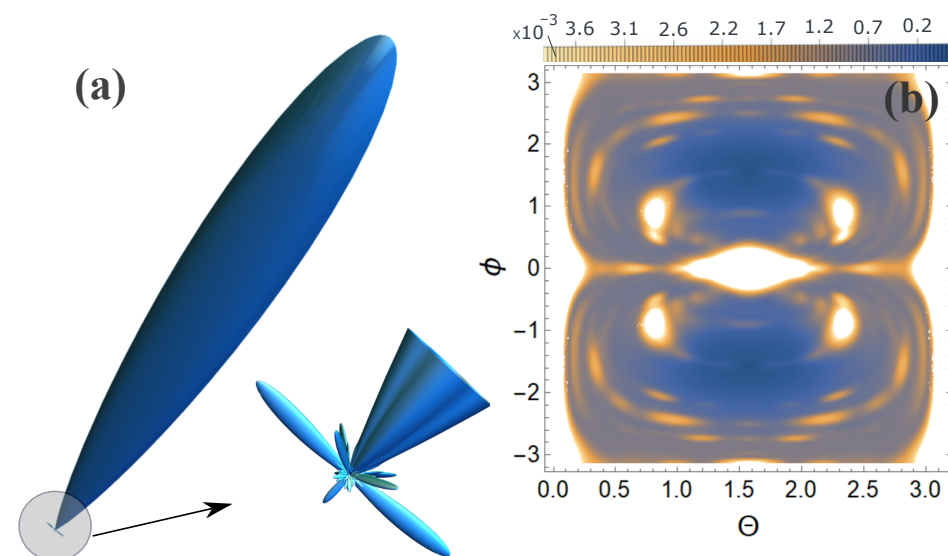


Figure 6. Same as in Figure 5 but for orientation 2; see Figure 2.

From Figures 5–8, it can be seen that the effect of the orientation of NV centers is indeed present despite the fact that the atomic composition and overall structure are preserved. However, this effect is not significant in relation to the main diffraction peaks (white spots on the 2D map). In order for this effect to be more noticeable and the effect of the orientation of NV centers to be clearly visible, it is necessary to consider not the scattering spectrum itself but the relative contribution of the scattering spectrum of the diamond lattice (without NV centers) and oriented NV centers normalized to the maximum value of the spectrum, i.e., $\delta = \left(\left[\frac{d\varepsilon}{d\Omega_{\mathbf{k}}} \right]_{NV} - \frac{d\varepsilon}{d\Omega_{\mathbf{k}}} \right) / \left[\frac{d\varepsilon}{d\Omega_{\mathbf{k}}} \right]_{max}$. The calculation results are presented in Figure 9.

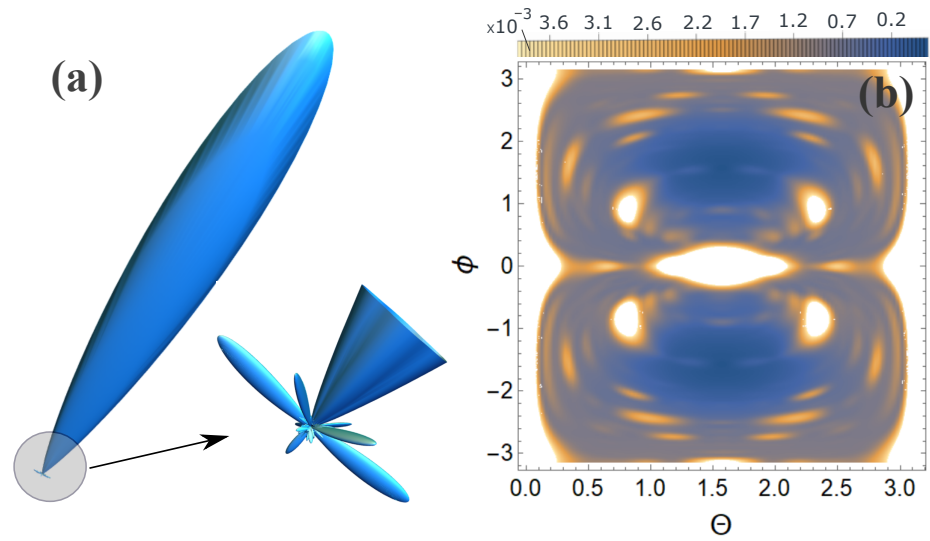


Figure 7. Same as in Figure 5, but for orientation 3; see Figure 3.

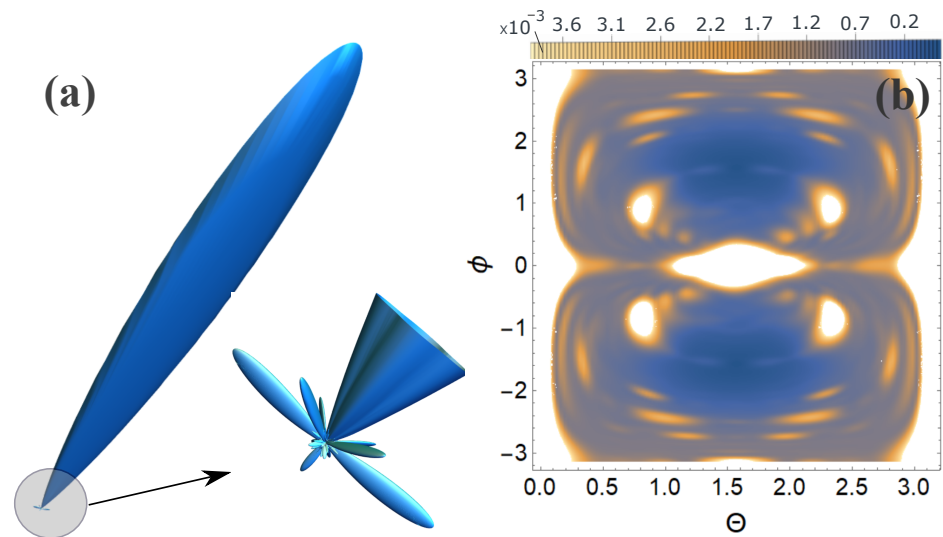


Figure 8. Same as in Figure 5 but for orientation 4; see Figure 4.

From Figure 9, it is clearly seen that there are differences in the scattering spectra with different orientations. These differences are clearly visible and may indicate the orientation of NV centers in the diamond structure.

In Figure 9a,b, you can see that the differences that arise in orientations 1 and 2 are almost symmetrical, but for orientations 3 and 4 (see Figure 9c,d), the differences become asymmetrical. This is primarily due to the direction between the incident pulse and the NV center. The most important thing is that there are such differences, which means the scattering spectra are sensitive to the orientation of the NV centers. It is also clear that all the patterns in Figure 9 are different, which means that the orientation of NV centers in the diamond structure can be determined from the pattern.

In these calculations, we considered the pulse to be ultrashort and took into account the pulse duration parameter τ . If we consider the momentum to be infinitely large $\tau \rightarrow \infty$ and take into account only the coherent term in Equation (2), then it will coincide with the previously well-known expression in the theory of diffraction analysis. Similar calculations were carried out, but at $\tau \rightarrow \infty$, it turned out that the error in using the previously known expression and the above calculations using Equation (2) large. This error is significantly larger than the studied effect of the orientation of NV centers. Thus, when using attosecond

pulses, when studying the effect of orientation of NV centers in the diamond structure from XRD theory, it is necessary to use the expression shown in Equation (2).

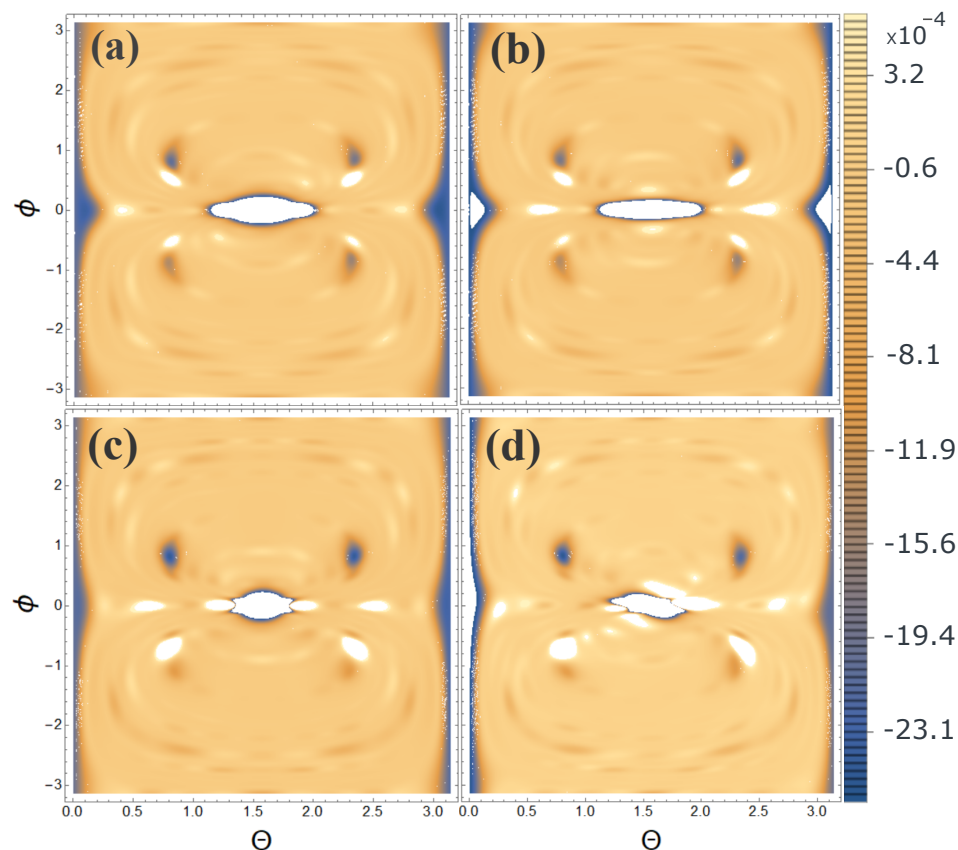


Figure 9. The calculation of the value $\delta = \left(\left[\frac{d\varepsilon}{d\Omega_{\mathbf{k}}} \right]_{NV} - \frac{d\varepsilon}{d\Omega_{\mathbf{k}}} \right) / \left[\frac{d\varepsilon}{d\Omega_{\mathbf{k}}} \right]_{max}$: (a) in the case of orientation 1, see Figure 1; (b) in case of orientation 2, see Figure 2; (c) in case of orientation 3, see Figure 3, (d) in case of orientation 4; see Figure 4.

3. Discussion and Conclusions

Thus, two important results were obtained in this work. The first result confirms the use of this theory (where the pulse duration is taken into account) and the large error of the previously developed and widely used theory (where the pulse duration is not taken into account) when using attosecond pulses. The second conclusion is the ability to determine the orientation of NV centers in the structure of the diamond lattice from scattering spectra.

In principle, when using ultrashort pulses, it is possible not only to determine the orientation of NV centers but also to determine the distances between planes with NV centers. Indeed, if we analyze the parameter $\gamma_{i,j}(\mathbf{p}_0, \mathbf{p}_\tau)$, then we can conclude that diffraction occurs when USP is scattered by atoms that are located inside space with length $\sim c\tau$. Thus, by manipulating the pulse duration, you can see that when the first and second planes begin to diffract, the spacing between the planes will be $\sim c\tau$. The same applies with a large number of planes. This technique for studying the structure of diamonds with NV centers is promising and will require additional study in the future.

It should be added that when studying NV centers in the structure of diamonds using USPs, it is necessary to take into account two well-known methods. The first technique is to collect information about a scattered USP on an oriented crystal relative to the direction of the incident USP, and the second technique is the pump-probe method, where the object under study is fed in a chaotic orientation relative to the incident pump and probe pulse. In general, the second technique is of interest for diamond nanocrystals (detonation diamonds, DND), the concentration of NV centers in which can be very high.

Author Contributions: Conceptualization, D.M. and M.E.; methodology, D.M. and V.M.; software, D.M., E.G., M.B. and K.M.; validation, D.M.; formal analysis, D.M. and M.E.; writing—original draft preparation, D.M. and M.E.; writing—review and editing, D.M.; project administration, D.M. and M.E. All authors have read and agreed to the published version of the manuscript.

Funding: The research was supported by grants from the Russian Science Foundation, No. 23-12-20014; state assignment of the Russian Federation, No. FSRU-2024-0005.

Data Availability Statement: Request to corresponding author of this article.

Conflicts of Interest: The authors declare no conflicts of interest.

References

1. Jones, N. Crystallography: Atomic secrets. *Nature* **2018**, *505*, 602–603. [[CrossRef](#)] [[PubMed](#)]
2. Benediktovich, A.; Feranchuk, I.; Ulyanekov, A. *Theoretical Concepts of X-ray Nanoscale Analysis*; Springer: Berlin/Heidelberg, Germany, 2014.
3. Eseev, M.K.; Matveev, V.I.; Makarov, D.N. Diagnostics of Nanosystems with the Use of Ultrashort X-ray Pulses: Theory and Experiment (Brief Review). *JETP Lett.* **2021**, *114*, 387–405. [[CrossRef](#)]
4. Krausz, F.; Ivanov, M. Attosecond physics. *Rev. Mod. Phys.* **2009**, *81*, 163. [[CrossRef](#)]
5. Dixit, G.; Vendrell, O.; Santra, R. Imaging electronic quantum motion with light. *Proc. Natl. Acad. Sci. USA* **2012**, *109*, 11636–11640. [[CrossRef](#)] [[PubMed](#)]
6. Calegari, F.; Sansone, G.; Stagira, S.; Vozzi, C.; Nisoli, M. Advances in attosecond science. *J. Phys. B At. Mol. Opt. Phys.* **2016**, *49*, 062001. [[CrossRef](#)]
7. Kraus, P.M.; Zürich, M.; Cushing, S.K.; Neumark, D.M.; Leone, S.R. The ultrafast X-ray spectroscopic revolution in chemical dynamics. *Nat. Rev. Chem.* **2018**, *2*, 82–94. [[CrossRef](#)]
8. Peng, P.; Marceau, C.; Villeneuve, D.M. Attosecond imaging of molecules using high harmonic spectroscopy. *Nat. Rev. Phys.* **2019**, *1*, 144–155. [[CrossRef](#)]
9. Schoenlein, R.; Elsaesser, T.; Holldack, K.; Huang, Z.; Kapteyn, H.; Murnane, M.; Woerner, M. Recent advances in ultrafast X-ray sources. *Philos. Trans. R. Soc. A* **2019**, *377*, 20180384. [[CrossRef](#)]
10. Duris, J.; Li, S.; Driver, T.; Champenois, E.G.; MacArthur, J.P.; Lutman, A.A.; Zhang, Z.; Rosenberger, P.; Aldrich, J.W.; Coffee, R.; et al. Tunable isolated attosecond X-ray pulses with gigawatt peak power from a free-electron laser. *Nat. Photonics* **2020**, *14*, 30–36. [[CrossRef](#)]
11. Maraju, P.K.; Grazioli, C.; Di Fraia, M.; Muioli, M.; Ertel, D.; Ahmadi, H.; Plekan, O.; Finetti, P.; Allaria, E.; Giannesi, L.; et al. Attosecond pulse shaping using a seeded free-electron laser. *Nature* **2020**, *578*, 386–391. [[CrossRef](#)]
12. Dunning, D.J.; McNeil, B.W.J.; Thompson, N.R. Few-Cycle Pulse Generation in an X-ray Free-Electron Laser. *Phys. Rev. Lett.* **2013**, *110*, 104801. [[CrossRef](#)]
13. Mukamel, S.; Healion, D.; Zhang, Y.; Biggs, J.D. Multidimensional attosecond resonant X-ray spectroscopy of molecules: Lessons from the optical regime. *Annu. Rev. Phys. Chem.* **2013**, *64*, 101–127. [[CrossRef](#)]
14. Balasubramanian, G.; Chan, I.Y.; Kolesov, R.; Al-Hmoud, M.; Tisler, J.; Shin, C.; Kim, C.; Wojcik, A.; Hemmer, P.R.; Krueger, A.; et al. Nanoscale imaging magnetometry with diamond spins under ambient conditions. *Nature* **2008**, *455*, 648–651. [[CrossRef](#)]
15. Doherty, M.W.; Manson, N.B.; Delaney, P.; Jelezko, F.; Wrachtrup, J.; Hollenberg, L.C. The nitrogen-vacancy colour centre in diamond. *Phys. Rep.* **2013**, *528*, 1–45. [[CrossRef](#)]
16. Barry, J.; Schloss, J.; Bauch, E.; Turner, M.; Hart, C.; Pham, L.; Walsworth, R. Sensitivity optimization for NV-diamond magnetometry. *Rev. Mod. Phys.* **2020**, *92*, 015004. [[CrossRef](#)]
17. Mrozek, M.; Schabikowski, M.; Mitura-Nowak, M.; Lekki, J.; Marszałek, M.; Wojciechowski, A.; Gawlik, W. Nitrogen-289 Vacancy Color Centers Created by Proton Implantation in a Diamond. *Materials* **2021**, *14*, 833. [[CrossRef](#)] [[PubMed](#)]
18. Popov, V.; Podlesny, S.; Kartashov, I.; Kupriyanov, I.; Palyanov, Y. Long dephasing time of NV center spins in diamond layers formed by hot ion implantation and high pressure high temperature annealing. *Diam. Relat. Mater.* **2021**, *120*, 108675. [[CrossRef](#)]
19. Pham, L.M.; Bar-Gill, N.; Le Sage, D.; Belthangady, C.; Stacey, A.; Markham, M.; Twitchen, D.J.; Lukin, M.D.; Walsworth, R.L. Enhanced metrology using preferential orientation of nitrogen-vacancy centers in diamond. *Phys. Rev. B* **2012**, *86*, 121202. [[CrossRef](#)]
20. Henriksen, N.E.; Moller, K.B. On the Theory of Time-Resolved X-ray Diffraction. *J. Phys. Chem. B* **2008**, *112*, 558–567. [[CrossRef](#)] [[PubMed](#)]
21. Astapenko, V.A.; Sakhno, E.V. Excitation of a quantum oscillator by short laser pulses. *Appl. Phys. B* **2020**, *126*, 23. [[CrossRef](#)]
22. Rosmej, F.B.; Astapenko, V.A.; Lisitsa, V.S.; Li, X.D.; Khramov, E.S. Scattering of ultrashort laser pulses on “ion-sphere” in dense plasmas. *Contrib. Plasma Phys.* **2019**, *59*, 189–196. [[CrossRef](#)]
23. Astapenko, V.A. Energy transfer from ultrashort electromagnetic pulses to a medium: From micro to macro description. *Phys. Lett. Sect. A Gen. At. Solid State Phys.* **2023**, *483*, 129050. [[CrossRef](#)]
24. Makarov, D.N. Quantum theory of scattering of ultrashort electromagnetic field pulses by polyatomic structures. *Opt. Express* **2019**, *27*, 31989–32008. [[CrossRef](#)] [[PubMed](#)]

25. Eseev, M.; Makarova, K.; Makarov, D. Scattering of Ultrashort X-ray Pulses on Diamonds with NV Centers. *Crystals* **2022**, *12*, 1417. [[CrossRef](#)]
26. Moller, K.B.; Henriksen, N.E. Time-resolved x-ray diffraction: The dynamics of the chemical bond. *Struct. Bond.* **2012**, *142*, 185.
27. Tanaka, S.; Chernyak, V.; Mukamel, S. Time-resolved x-ray spectroscopies: Nonlinear response functions and liouville-space pathways. *Phys. Rev. A* **2001**, *63*, 63405–63419. [[CrossRef](#)]
28. Dixit, G.; Slowik, J.; Santra, R. Proposed Imaging of the Ultrafast Electronic Motion in Samples using X-ray Phase Contrast. *Phys. Rev. Lett.* **2013**, *110*, 137403. [[CrossRef](#)] [[PubMed](#)]
29. James, R.W. *The Optical Principles of the Diffraction of X-rays (Ox Bow)*; Ox Bow Press: Woodbridge, CT, USA, 1982.
30. Makarov, D.N.; Makarova, K.A.; Kharlamova, A.A. Specificity of scattering of ultrashort laser pulses by molecules with polyatomic structure. *Sci. Rep.* **2022**, *12*, 4976. [[CrossRef](#)]
31. Makarov, D.; Kharlamova, A. Scattering of Attosecond Laser Pulses on a DNA Molecule during Its Nicking and Bending. *Int. J. Mol. Sci.* **2023**, *24*, 15574. [[CrossRef](#)]
32. Makarov, D.N.; Eseev, M.K.; Makarova, K.A. Analytical wave function of an atomic electron under the action of a powerful ultrashort electromagnetic field pulse. *Opt. Lett.* **2019**, *44*, 3042–3045. [[CrossRef](#)]
33. Abbey, B.; Dilanian, R.A.; Darmanin, C.; Ryan, R.A.; Putkunz, C.T.; Martin, A.V.; Wood, D.; Streltsov, V.; Jones, M.W.; Gaffney, N.; et al. X-ray laser-induced electron dynamics observed by femtosecond diffraction from nanocrystals of Buckminsterfullerene. *Sci. Adv.* **2016**, *2*, e1601186. [[CrossRef](#)] [[PubMed](#)]
34. Salvat, F.; Martinez, J.D.; Mayol, R.; Parellada, J. Analytical Dirac-Hartree-Fock-Slater screening function for atoms ($Z = 1-92$). *Phys. Rev. A* **1987**, *36*, 467–474. [[CrossRef](#)] [[PubMed](#)]
35. Lin, Q.; Zheng, J.; Becker, W. Subcycle pulsed focused vector beams. *Phys. Rev. Lett.* **2006**, *97*, 253902. [[CrossRef](#)] [[PubMed](#)]

Disclaimer/Publisher's Note: The statements, opinions and data contained in all publications are solely those of the individual author(s) and contributor(s) and not of MDPI and/or the editor(s). MDPI and/or the editor(s) disclaim responsibility for any injury to people or property resulting from any ideas, methods, instructions or products referred to in the content.